NANO LETTERS
Cite This: Nano Lett. 2018, 18, 152−157
Letter
pubs.acs.org/NanoLett

Near-Field Enhanced Photochemistry of Single Molecules in a Scanning Tunneling Microscope Junction

Hannes Böckmann,[†] Sylwester Gawinkowski,[‡] Jacek Waluk,[‡,§] Markus B. Raschke,[∥] Martin Wolf,[†] and Takashi Kumagai*[,†,⊥]

[†]Department of Physical Chemistry, Fritz-Haber Institute of the Max-Planck Society, Faradayweg 4-6, 14195 Berlin, Germany
[‡]Institute of Physical Chemistry, Polish Academy of Sciences, Kasprzaka 44/52, Warsaw 01-224, Poland
[§]Faculty of Mathematics and Natural Sciences, College of Science, Cardinal Stefan Wyszyński University, Dewajtis 5, 01-815 Warsaw, Poland
[∥]Department of Physics, Department of Chemistry, and JILA, University of Colorado, Boulder, Colorado 80309, United States
[⊥]JST-PRESTO, 4-1-8 Honcho, Kawaguchi, Saitama 332-0012, Japan

Supporting Information

ABSTRACT: Optical near-field excitation of metallic nanostructures can be used to enhance photochemical reactions. The enhancement under visible light illumination is of particular interest because it can facilitate the use of sunlight to promote photocatalytic chemical and energy conversion. However, few studies have yet addressed optical near-field induced chemistry, in particular at the single-molecule level. In this Letter, we report the near-field enhanced tautomerization of porphycene on a Cu(111) surface in a scanning tunneling microscope (STM) junction. The light-induced tautomerization is mediated by photogenerated carriers in the Cu substrate. It is revealed that the reaction cross section is significantly enhanced in the presence of a Au tip compared to the far-field induced process. The strong enhancement occurs in the red and near-infrared spectral range for Au tips, whereas a W tip shows a much weaker enhancement, suggesting that excitation of the localized plasmon resonance contributes to the process. Additionally, using the precise tip−surface distance control of the STM, the near-field enhanced tautomerization is examined in and out of the tunneling regime. Our results suggest that the enhancement is attributed to the increased carrier generation rate via decay of the excited near-field in the STM junction. Additionally, optically excited tunneling electrons also contribute to the process in the tunneling regime.

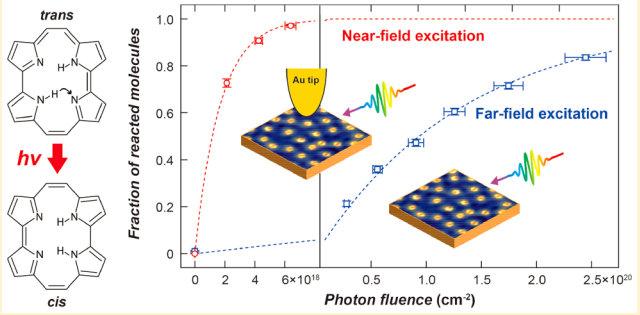

KEYWORDS: *Near-field induced reaction, tautomerization, single molecule, metal surface, scanning tunneling microscopy*

Optical excitations of molecules mediated by metallic nanostructures have a wide range of applications such as surface-enhanced Raman spectroscopy (SERS),[1] enhanced molecular luminescence,[2] and photocatalysis.[3] Additionally, tip-enhanced Raman spectroscopy (TERS) has recently emerged as a powerful tool for single-molecule spectroscopy.[4−6] On the other hand, enhancement of photochemical reactions is of particular interest for efficient conversion of light into chemical energy. Nanostructures made of Au, Ag, and Cu are commonly employed as a photocatalytic substrate because of plasmonic resonances in the visible and near-infrared spectral range, which can facilitate the use of sunlight to enhance photochemical reactions.[10] Photochemical reactions at nanostructure interfaces induced through near-field excitation can occur by the following mechanisms: direct excitation of molecular adsorbates (electric−dipole transition), charge transfer within hybridized adsorbate−substrate states via plasmon relaxation to electron−hole pair excitation, or local heating due to hot carrier relaxation.[8−12] While these excitation mechanisms have been established for photochemical reactions on single-crystalline metal surfaces by far-field excitation,[13−15] it has been found that the reactions can also be enhanced through near-field excitation on plasmonic nanostructures and most effectively in nanoscale gaps.[3] However, it has remained a very challenging task to investigate near-field induced reactions in individual nanogaps with spectroscopic methods on the molecular level. The near-field properties in nanogaps are of fundamental importance and the gap distance is a dominant parameter determining resonance energy and degree of field enhancement. Recent theoretical and experimental studies have revealed that the near-field properties are affected by electron tunneling at subnanometer gap distances,[16−25] where the classical electrodynamics description fails to describe the near-field properties. However, the gap distance dependence of

Received: August 29, 2017
Revised: November 29, 2017
Published: December 21, 2017

DOI: 10.1021/acs.nanolett.7b03720
Nano Lett. 2018, 18, 152−157

near-field induced reactions notably in that transition regime has not yet been studied in a controlled manner. A low-temperature STM is a powerful tool to directly study chemical reactions of individual adsorbates[26,27] in (sub)nanometer tunneling junctions with precise control of the tip−sample distance. Therefore, STM experiments combined with photoexcitation can be used to study near-field induced processes within a single nanogap. However, to date most of surface photochemical reactions of single adsorbates have been examined by far-field excitation[28−40] with yet limited effort on near-field induced reactions in an STM junction.[41−43] Here, we present a systematic study of tip-enhanced tautomerization of single porphycene molecules on Cu(111), investigated with a low-temperature STM combined with variable wavelength excitation.

Porphycene molecules adsorb on Cu(111) either in the thermodynamically stable trans or metastable cis configuration (Figure 1a). All of the molecules were observed in the trans configuration at 5 K after deposition onto the Cu(111) surface at room temperature. The unidirectional trans → cis tautomerization can be induced by injection of energetic electrons from the STM tip[44] or exposing the surface to light.[45] The backward cis → trans conversion can be induced selectively by heating the surface and all cis molecules can be converted to the trans configuration above ∼35 K.[44] We previously showed that the STM- and light-induced tautomerization occurs via attachment of hot carriers followed by vibrational excitation of the molecule[44,45] and proposed that the unidirectional tautomerization could be rationalized by the stability inversion between the trans and cis configuration upon vibrational excitation of a skeletal mode of porphycene.[45] Recently, the tautomerization mechanism of porphycene on Cu(111) was theoretically investigated. Novko et al. demonstrated that the tautomerization coordinate (potential energy surface) is deformed by the excitation of skeletal vibrational modes via electron attachment, which indeed leads to the reversed stability between the trans and cis configurations and consequently the unidirectional conversion.[46] The simulation also found that the electric field perpendicular to the surface does not significantly affect the tautomerization coordinate and cannot be a driving force of the reaction.

Here we find that the light-induced tautomerization can be locally enhanced in the presence of a metallic tip. Figure 1b shows STM images at 5 K before and after irradiation by 720 nm light in the presence of a Au tip positioned at the center of the image. The tip was fixed in the tunneling regime at I_t = 30 pA and V_{bias} = 50 mV. The incident beam angle was 65° with respect to surface normal and polarized along the tip axis (p-polarized). This voltage is well below the threshold for tunneling electron-induced tautomerization (∼150 mV[44,45]). After irradiation, the molecules near the tip are converted from the trans to cis configuration. To avoid tip−sample contact and unwanted damage of the tip/surface due to thermal expansion of the tip,[47] we used a relatively low photon flux (∼10^{15}−10^{16} photons/cm^2/s). This allows to compensating the thermal expansion by the STM feedback loop, so that the tip−surface distance could be kept constant during light irradiation. The sample temperature was raised from 5.2 to 6−7 K upon irradiation (the temperature variation depends on the excitation wavelength and the irradiance used). As mentioned above, surface heating leads to the selective cis → trans conversion.[44] Therefore, if thermal contributions to the photoinduced tautomerization were significant during light irradiation, the complete conversion of all porphycene molecules to the cis configuration should be impeded due to the competing cis → trans conversion. However, the complete light-induced conversion to the cis configuration after sufficient irradiance (cf. Figure 2a and ref 45) indicates a negligible role of the thermally activated process.

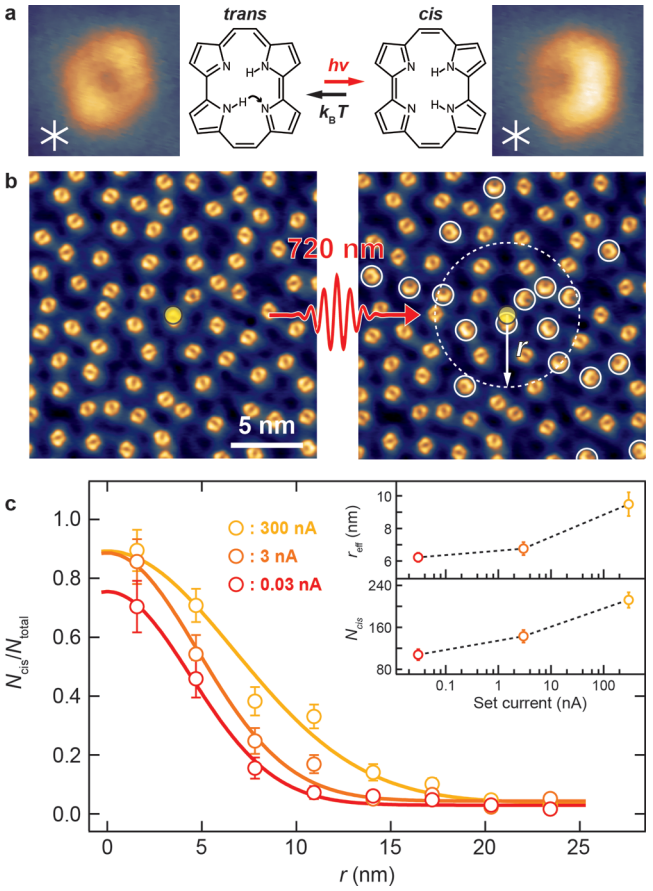

Figure 1. Tip-enhanced light-induced tautomerization of porphycene on Cu(111) with a Au tip. (a) STM images and chemical structures of porphycene in the trans and cis configuration. (b) STM images (5 K, V_{bias} = 50 mV, and I_t = 30 pA, scan size: 25 × 25 nm^2) before (left) and after (right) illumination at 720 nm light with n_{ph} = (2.9 ± 0.2) × 10^{17} cm^{-2}. The Au tip is located at the center of the image (indicated by a yellow circle). The molecules converted to the cis configuration are marked by white circles. (c) Radial distribution of the trans → cis conversion probability measured at three different tip−surface distances, as determined by the STM set-point (V_{bias} = 50 mV with set-currents indicated in the figure). The solid lines represent the best fit to a Gaussian, $A \exp\left(-\frac{r^2}{2\sigma^2}\right)$, where $\sigma = r_{eff}$. Assuming the decay constant of the tunneling current of ∼11 nm^{-1},[52] the variation of the set-current from 0.03 to 300 nA corresponds to a relative tip height displacement of approximately 4 Å. Inset shows set-current (tip-height) dependence of r_{eff} (top) and N_{cis} (bottom) (dashed lines are a guide to the eye).

Figure 1c displays the radial distributions of the tautomerization probability as a function of the radial distance from the central tip position, obtained from repeated measurements (about 1200 molecules were counted in total) and measured at different tip−surface distances. The radial decay reveals a strong enhancement within ∼10 nm radius, which is consistent with the expected range of the near-field localization in the

DOI: 10.1021/acs.nanolett.7b03720
Nano Lett. 2018, 18, 152−157

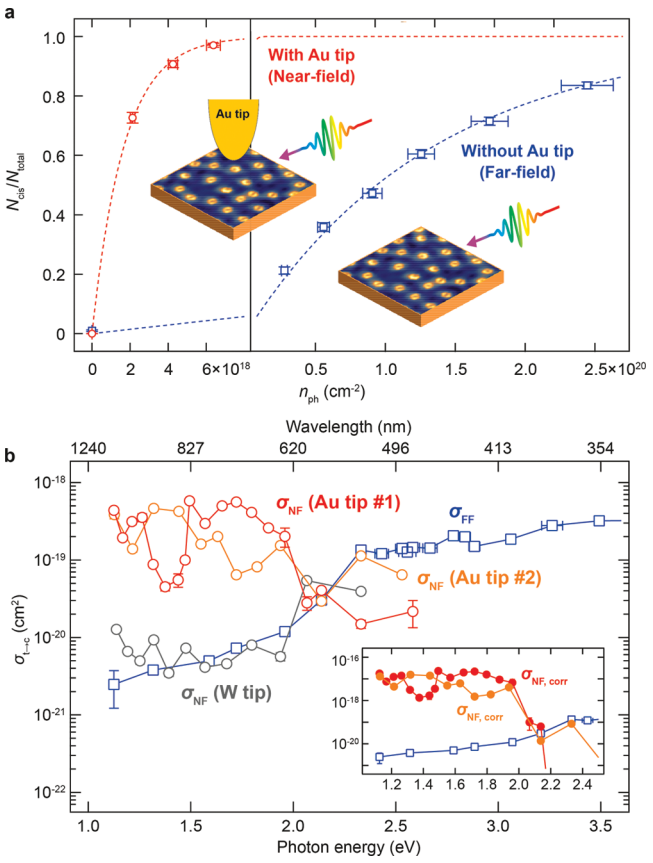

Figure 2. Cross section of the trans → cis tautomerization. (a) Fraction of the cis molecules reacted under illumination by 720 nm light as a function of photon fluence, measured with (circles) and without (squares) a Au tip. The near-field data were obtained while scanning the Au tip over the surface (60 × 60 nm^2, 580 molecules) at the set point of I_t = 30 pA and V_{bias} = 50 mV. The dashed curves represent the best fitted results of the data to a first-order rate equation, eq 1. (b) Wavelength dependence of the cross section for near-field excitation obtained for two different Au tips (red and orange circles) and a W tip (gray circles), in comparison to the far-field cross sections (squares).[45] The near-field data were obtained with the set point of I_t = 30 pA and V_{bias} = 50 mV. The inset shows the corrected cross sections for the Au tips, by applying eq 2.

STM junction.[48−51] We estimate r_{eff} by fitting the distribution to an exponential decay function[50] and find that r_{eff} and the total number of the reacted molecules (N_{cis}) increase with decreasing tip−surface distance (see inset of Figure 1c).

In order to quantify the tip-enhancement effect, we investigated the tautomerization cross section in the presence and absence of a metallic tip, that is, comparing near-field and far-field excitation. In the near-field experiment, the STM junction was illuminated while scanning across the surface (60 × 60 nm^2) in the constant current mode. In this scan area, a statistically sufficient number of molecules (~600 molecules) were probed to determine the reaction cross section. In the far-field experiments, the tip was retracted by 2−3 μm from the surface during illumination in order to exclude any influence from the tip to the reaction. Figure 2a shows the resulting evolution of the cis molecule fraction as a function of photon fluence at the excitation wavelength of 720 nm (far- and near-field experiments using the Au tip). The cross section of the trans → cis tautomerization ($\sigma_{t\to c}$) is obtained by fitting the evolution to a first-order rate equation

$$\frac{N_{cis}}{N_{total}} = 1 - \exp(-\sigma_{t\to c} n_{ph}) \quad (1)$$

where N_{cis} is the number of cis molecules (reacted), N_{total} the total number of molecules in the scanned area, and n_{ph} the photon fluence in photons per cm^2. At 720 nm we find $\sigma_{t\to c}$ = (5.59 ± 0.35) × 10^{-19} and (7.27 ± 0.18) × 10^{-21} cm^2 for near- and far-field excitation, respectively. Hence, the presence of the Au tip dramatically enhances the tautomerization through near-field excitation in the junction.

The same measurements were then repeated for different excitation wavelengths to investigate the wavelength dependence of the near-field induced tautomerization. The evolution of the trans → cis conversion follows a first order process at all wavelengths. We measured the wavelength dependence with different Au tips, one W, and one PtIr (80:20) tip (see Supporting Information for the radial dependence of the enhancement with the W, PtIr and the other Au tips, Figure S1). Figure 2b shows the corresponding wavelength (photon energy) dependence of the measured cross sections for both far- and near-field excitation and for the Au and W tips (see Supporting Information for the PtIr tip, Figure S2). A large enhancement is observed for the Au and PtIr tips, but only a small effect is seen for the W tip.

We note a likely underestimation of the measured cross sections in the near-field experiments in the wavelength range where a significant enhancement occurs (i.e., $\sigma_{NF} \gg \sigma_{FF}$). As described above, the tip was scanned across the surface in the near-field experiments in order to determine the cross section. However, the scan area (A_{scan}) of 60 × 60 nm^2 is substantially larger than the effective size of the enhancement spot (cf. Figure 1). This leads to an apparent reduction of the actual cross section. The corrected near-field cross section $\sigma_{NF,corr}$ can be calculated from the measured cross section σ_{NF} by the following equation (see Supporting Information)

$$\sigma_{NF,corr} \approx \left(\frac{A_{scan} + 2\sqrt{\pi A_{scan}}\, r + \pi r^2}{\pi r^2} \right)^{1-\sigma_{FF}/\sigma_{NF}} \cdot \sigma_{NF} \quad (2)$$

where r is the effective radius (r_{eff}) of the enhancement spot which is estimated to be 6.2 ± 0.3 nm from the conversion probability profile for the Au tip in Figure 1c. According to eq 2, the measured σ_{NF} for the Au tip corresponds to only about 2.4% of the actual cross section when the near-field process is dominant ($\sigma_{NF} \gg \sigma_{FF}$). The inset of Figure 2b shows the corrected near-field cross sections, $\sigma_{NF,corr}$ for the Au tips. However, we did not apply the correction for the W tip because of the weak enhancement (σ_{NF} is comparable with σ_{FF}).

The wavelength-dependent cross section of the far-field excitation in Figure 2b is explained by a dominant contribution of the substrate-mediated (indirect) mechanism, as reported previously.[45] This is reflected in a rapid increase of the far-field cross section up to ~2.3 eV, which is attributed to the excitation of d-band electrons of the Cu substrate. On the other hand, the near-field cross sections are largely increased with the Au tips in the red and near-infrared range (620−1100 nm) and the ratio between $\sigma_{NF,corr}$ and σ_{FF}, that is, the enhancement factor, reaches ~10^2−10^3. The spectral regime where strong enhancement takes place matches the energy range of the localized plasmon resonance of a Au tip, leading to a strong field enhancement.[53,54] In contrast, a W tip does not support localized plasmons in this wavelength region and the

DOI: 10.1021/acs.nanolett.7b03720
Nano Lett. 2018, 18, 152−157

field enhancement is much weaker than for Au tips.[53,54] Additionally, the wavelength-dependent cross section shows significant tip-to-tip variation for different Au tips, indicating that the spectral response is not correlated with the properties of porphycene and the Cu substrate but associated with structural details of the tip apex which determine the near-field response. However, the strong reduction of the enhancement occurs for both Au tips around 2 eV, which can be explained by quenching of the near-field excitation due to interband absorption of the Au tip/Cu substrate.[55] Further quantitative description and modeling of the near-field properties were impossible due to the lack of detailed information about the tip structure. It should be noted that we carried out in situ tip preparations such as application of voltage pulses and controlled indentation of the tip into the surface (it was necessary to obtain an adequate resolution to distinguish between the trans and cis configurations). Therefore, the tip apex may contain Cu atoms from the surface.

Figure 3a shows the tip−surface distance dependence of the cross section measured in the tunneling regime at different wavelengths for the Au tip #1. At 720 nm, the cross section increases as the tip approaches the surface. It shows only a very

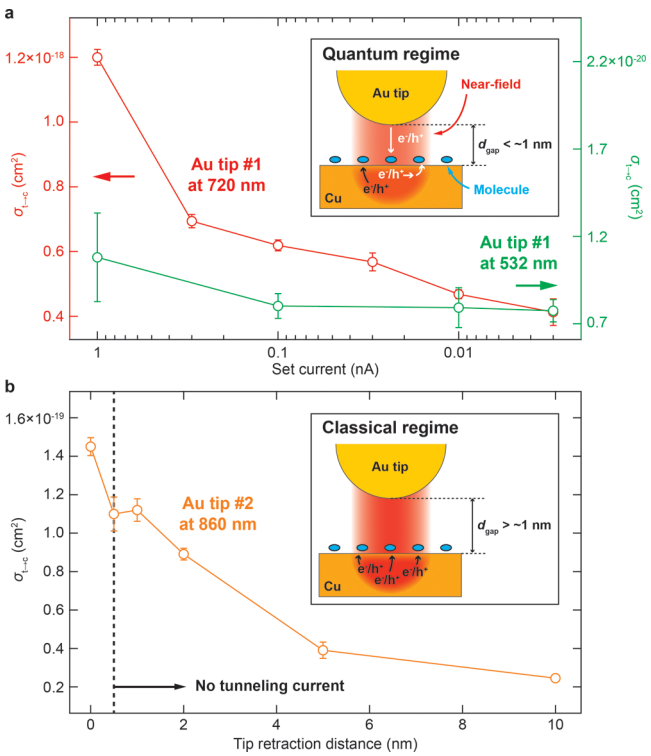

Figure 3. Gap distance dependence of near-field induced tautomerization. (a) The tip−surface distance-dependent cross sections measured in the tunneling regime at 720 nm (red circles) and 532 nm (green circles) with Au tip #1. (b) Tip−surface distance dependent cross sections outside the tunneling regime measured at 860 nm with Au tip #2. The tip is vertically retracted from the set-point of V_{bias} = 50 mV and I_t = 30 pA (zero-point in the horizontal axis) with the feedback loop disabled. After retraction, the tip was scanned across the surface (60 × 60 nm^2, about 670 molecules) under illumination. The reacted molecules were identified in the images, taken after the illumination. In order to minimize the relative displacement between the tip and the surface during illumination, a very low photon flux of (3.9 ± 0.3)−(9.6 ± 0.6) × 10^{15} cm^{-2}s^{-1} was used.

weak dependence at 532 nm, with lower cross section as expected because of quenching via interband transitions. We found that the efficiency of the near-field induced tautomerization does not decay with decreasing the gap distance between a Au tip and the surface in the tunneling regime (Figure 1c and Figure 3a). We also examined the tip-enhanced tautomerization at larger gap distances up to ∼10 nm where electron tunneling is negligible. Figure 3b shows the gap distance dependence of the measured σ_{NF} at 860 nm excitation with the Au tip #2. The gap distance is defined by the retraction distance of the tip from the set-point of V_{bias} = 50 mV and I_t = 30 pA (corresponding to the zero-point). No tunneling current was detected at retraction distances greater than 0.5 nm.

We tentatively explain that the near-field enhanced tautomerization results from the increased carrier generation rate in the Cu substrate via decay of the excited near-field in the STM junction. The process involves two different regimes separated by the existence of electron tunneling between the tip and the surface (inset of Figure 3a,b). At relatively large gap distances (classical regime), the reaction is dominated by the localized generation of hot carriers in the Cu substrate. On the other hand, tunneling electrons generated by the optical excitation may contribute to the process in the tunneling (quantum) regime. As reported previously,[44] tunneling electrons from the STM can also induce the unidirectional trans → cis tautomerization, which occurs "non-locally", that is, not only just under the tip, but also in molecules away from the STM tip due to hot carrier transport along the surface. However, electron tunneling can significantly reduce the local field enhancement.[16] Our results show the increase of the cross section with decreasing the gap distance in the tunneling regime (Figure 3a). This may suggest that the process induced by optically excited tunneling electrons overcompensates the reduction of the field enhancement. It should also be mentioned that the interaction between the near-field and molecules scales differently from the net field enhancement and could increase continuously in the tunneling regime.[24] For instance, it was observed that TERS signal shows a continuous increase with decreasing a gap distance of an STM junction even in the tunneling regime.[5,24] Vibrational excitation through Raman scattering could also contribute to the reaction.[43]

Electron tunneling also leads to the progressive transition of the resonance from bonding dimer plasmon to tunneling charge transfer plasmon around a threshold tunneling distance (∼0.5 nm).[16,18,21] The near-field enhancement of the tautomerization observed in the red and near-infrared regime for the Au tips (Figure 2b) may be assigned to the excitation of the superposition of these and the fundamental classical plasmon modes.

In summary, near-field enhanced tautomerization of porphycene on Cu(111) was directly observed using a low-temperature STM combined with wavelength tunable laser excitation. It was revealed that a significant enhancement occurs for Au tips in the red and near-infrared range, whereas the enhancement is weak for a W tip, indicating that excitation of localized plasmon resonances results in the strong enhancement. The near-field induced tautomerization was examined in and out of the tunneling regime. Our results suggest that the near-field enhanced process is dominated by photogenerated carriers in the Cu substrate which is locally enhanced via decay of the excited near-field in the STM junction. Additionally, optically excited tunneling electrons

DOI: 10.1021/acs.nanolett.7b03720
Nano Lett. 2018, 18, 152−157

between tip and surface may contribute to the process in the tunneling regime.

The presented work demonstrates a new possibility to study directly near-field enhanced chemistry at the single-molecule level in a (sub)nanometer gap with precise control of the gap distance. Because both optical field and hot carrier dynamics, which dominate the photochemical processes on metallic surfaces, are sensitive to the structural details of a nanogap and molecular configuration therein, a microscopic understanding of the reaction mechanism is still outstanding and necessary for an optimal design of plasmonic photocatalysts. Studies of single-molecule photochemical reactions using a controlled nanogap of STM in a well-defined environment can provide important fundamental insights. Additionally, single-molecule tautomerization has been demonstrated to act as a single-molecule switch in molecular scale electronics, which can be activated by various different external stimuli.[56−60] Our results suggest a new possibility for a near field-responsive molecular switch.

Experiments. All experiments were performed in an ultrahigh vacuum chamber (base pressure of $<10^{-10}$ mbar), equipped with a low-temperature STM (modified Omicron instrument with Nanonis Electronics). STM measurements were carried out at 5 K and the images were acquired in the constant current mode. The bias voltage was applied to the sample (denoted as V_{bias}). A Cu(111) surface was cleaned by repeated cycles of argon ion sputtering and annealing to 700−800 K. The STM tips were made from polycrystalline Au and W wires by electrochemical etching. Porphycene molecules were deposited from a Knudsen cell (at an evaporation temperature of 450−500 K). For illumination, a wavelength tunable laser (NKT Photonics) was used with a spectral bandwidth of 6−8 nm in the red and near-infrared range with a maximum power of a few mW. In order to avoid systematic errors caused by misalignment of the relative position between the STM and the beam spot, the laser beams were shaped into a 2−3 mm top-hat square before coupling them to the STM junction (see Supporting Information of ref 45).

■ ASSOCIATED CONTENT

Supporting Information

The Supporting Information is available free of charge on the ACS Publications website at DOI: 10.1021/acs.nanolett.7b03720.

Radial Distribution of trans → cis conversion probability with PtIr, W, and Au tips. Wavelength dependence of the near-field induced tautomerization for the PtIr tip. Derivation of corrected near-field cross section (PDF)

■ AUTHOR INFORMATION

Corresponding Author

*E-mail: kuma@fhi-berlin.mpg.de.

ORCID

Takashi Kumagai: 0000-0001-7029-062X

Notes

The authors declare no competing financial interest.

■ ACKNOWLEDGMENTS

T.K. acknowledges the support by JST-PRESTO (JPMJPR16S6). J.W. acknowledges the support by the Polish National Science Center Grants (2016/22/A/ST4/00029 and 2013/10/M/ST4/00069). M.B.R. acknowledges support from the Alexander Humboldt foundation, and funding from the National Science Foundation (NSF Grant CHE 1709822).

■ REFERENCES

(1) Kneipp, K.; Moskovits, M.; Kneipp, H. *Surface-Enhanced Raman Scattering*; Springer-Verlag: Berlin Heidelberg 2006.
(2) Tam, F.; Goodrich, G. P.; Johnson, B. R.; Halas, N. J. *Nano Lett.* **2007**, *7* (2), 496−501.
(3) Linic, S.; Aslam, U.; Boerigter, C.; Morabito, M. *Nat. Mater.* **2015**, *14*, 567−576.
(4) Pettinger, B.; Schambach, P.; Villagómez, C. J.; Scott, N. *Annu. Rev. Phys. Chem.* **2012**, *63*, 379−99.
(5) Zhang, R.; Zhang, Y.; Dong, Z. C.; Jiang, S.; Zhang, C.; Chen, L. G.; Zhang, L.; Liao, Y.; Aizpurua, J.; Luo, Y.; Yang, J. L.; Hou, J. G. *Nature* **2013**, *498*, 82−86.
(6) Jiang, N.; Kurouski, D.; Pozzi, E. A.; Chiang, N.; Hersam, M. C.; Van Duyne, R. P. *Chem. Phys. Lett.* **2016**, *659*, 16−24.
(7) Christopher, P.; Xin, H.; Linic, S. *Nat. Chem.* **2011**, *3*, 467−472.
(8) Boerigter, C.; Campana, R.; Morabito, M.; Linic, S. *Nat. Commun.* **2016**, *7*, 10545.
(9) Kim, K. H.; Watanabe, K.; Mulugeta, D.; Freund, H.-J.; Menzel, D. *Phys. Rev. Lett.* **2011**, *107*, 047401.
(10) Mulugeta, D.; Kim, K. H.; Watanabe, K.; Menzel, D.; Freund, H.-J. *Phys. Rev. Lett.* **2008**, *101*, 146103.
(11) Christopher, P.; Xin, H.; Marimuthu, A.; Linic, S. *Nat. Mater.* **2012**, *11*, 1044−1050.
(12) Mukherjee, S.; Libisch, F.; Large, N.; Neumann, O.; Brown, L. V.; Cheng, J.; Lassiter, J. B.; Carter, E. A.; Nordlander, P.; Halas, N. J. *Nano Lett.* **2013**, *13* (1), 240−247.
(13) Zhou, X.-L.; Zhu, X.-Y.; White, J. M. *Surf. Sci. Rep.* **1991**, *13* (3), 73−220.
(14) Zimmermann, F. M.; Ho, W. *Surf. Sci. Rep.* **1995**, *22* (4), 127−247.
(15) Lindstrom, C. D.; Zhu, X.-Y. *Chem. Rev.* **2006**, *106* (10), 4281−4300.
(16) Zuloaga, J.; Prodan, E.; Nordlander, P. *Nano Lett.* **2009**, *9* (2), 887−891.
(17) Pérez-González, O.; Zabala, N.; Borisov, A. G.; Halas, N. J.; Nordlander, P.; Aizpurua, J. *Nano Lett.* **2010**, *10* (8), 3090−3095.
(18) Savage, K. J.; Hawkeye, M. M.; Esteban, R.; Borisov, A. G.; Aizpurua, J.; Baumberg, J. J. *Nature* **2012**, *491*, 574−577.
(19) Marinica, D. C.; Kazansky, A. K.; Nordlander, P.; Aizpurua, J.; Borisov, A. G. *Nano Lett.* **2012**, *12* (3), 1333−1339.
(20) Esteban, R.; Borisov, A. G.; Nordlander, P.; Aizpurua, J. *Nat. Commun.* **2012**, *3*, 825.
(21) Scholl, J. A.; García-Etxarri, A.; Koh, A. L.; Dionne, J. A. *Nano Lett.* **2013**, *13* (2), 564−569.
(22) Zhu, W.; Crozier, K. B. *Nat. Commun.* **2014**, *5*, 5228.
(23) Hajisalem, G.; Nezami, M. S.; Gordon, R. *Nano Lett.* **2014**, *14* (11), 6651−6654.
(24) Kravtsov, V.; Berweger, S.; Atkin, J. M.; Raschke, M. B. *Nano Lett.* **2014**, *14* (9), 5270−5275.
(25) Zhu, W.; Esteban, R.; Borisov, A. G.; Baumberg, J. J.; Nordlander, P.; Lezec, H. J.; Aizpurua, J.; Crozier, K. B. *Nat. Commun.* **2016**, *7*, 11495.
(26) Ho, W. *J. Chem. Phys.* **2002**, *117*, 11033.
(27) Kim, Y.; Motobayashi, K.; Frederiksen, T.; Ueba, H.; Kawai, M. *Prog. Surf. Sci.* **2015**, *90*, 85−238.
(28) Bartels, L.; Wang, F.; Möller, D.; Knoesel, E.; Heinz, T. F. *Science* **2004**, *305*, 648−651.
(29) Comstock, M. J.; Levy, N.; Kirakosian, A.; Cho, J.; Lauterwasser, F.; Harvey, J. H.; Strubbe, D. A.; Fréchet, J. M. J.; Trauner, D.; Louie, S. G.; Crommie, M. F. *Phys. Rev. Lett.* **2007**, *99*, 038301.
(30) Comstock, M. J.; Levy, N.; Cho, J.; Berbil-Bautista, L.; Crommie, M. F.; Poulsen, D. A.; Fréchet, J. M. J. *Appl. Phys. Lett.* **2008**, *92*, 123107.

DOI: 10.1021/acs.nanolett.7b03720
Nano Lett. 2018, 18, 152−157

(31) Levy, M.; Comstock, M. J.; Cho, J.; Berbil-Bautista, L.; Kirakosian, A.; Lauterwasser, F.; Poulsen, D. A.; Fréchet, J. M. J.; Crommie, M. F. *Nano Lett.* **2009**, *9*, 935−939.
(32) Comstock, M. J.; Strubbe, D. A.; Berbil-Bautista, L.; Levy, N.; Cho, J.; Poulsen, D.; Fréchet, J. M. J.; Louie, S. G.; Crommie, M. F. *Phys. Rev. Lett.* **2010**, *104*, 178301.
(33) Bazarnik, M.; Henzl, J.; Czajka, R.; Morgenstern, K. *Chem. Commun.* **2011**, *47*, 7764−7766.
(34) Henzl, J.; Puschnig, P.; Ambrosch-Draxl, C.; Schaate, A.; Ufer, B.; Behrens, P.; Morgenstern, K. *Phys. Rev. B: Condens. Matter Mater. Phys.* **2012**, *85*, 035410.
(35) Bazarnik, M.; Jurczyszyn, L.; Czajka, R.; Morgenstern, K. *Phys. Chem. Chem. Phys.* **2015**, *17*, 5366.
(36) Bronner, C.; Schulze, G.; Franke, K. J.; Pascual, J. I.; Tegeder, P. *J. Phys.: Condens. Matter* **2011**, *23*, 484005.
(37) Schulze, G.; Franke, K. J.; Pascual, J. I. *Phys. Rev. Lett.* **2012**, *109*, 026102.
(38) Mehlhorn, M.; Carrasco, J.; Michaelides, A.; Morgenstern, K. *Phys. Rev. Lett.* **2009**, *103*, 026101.
(39) Zaum, Ch.; Meyer-auf-der-Heide, K. M.; Mehlhorn, M.; McDonough, S.; Schneider, W. F.; Morgenstern, K. *Phys. Rev. Lett.* **2015**, *114*, 146104.
(40) Mehlhorn, M.; Gawronski, H.; Morgenstern, K. *Phys. Rev. Lett.* **2010**, *104*, 076101.
(41) Wu, S. W.; Ogawa, N.; Ho, W. *Science* **2006**, *312*, 1362−1365.
(42) Tallarida, N.; Rios, L.; Apkarian, V. A.; Lee, J. *Nano Lett.* **2015**, *15*, 6386−6394.
(43) Li, S.; Chen, S.; Li, J.; Wu, R.; Ho, W. *Phys. Rev. Lett.* **2017**, *119*, 176002.
(44) Ladenthin, J. N.; Grill, L.; Gawinkowski, S.; Liu, S.; Waluk, J.; Kumagai, T. *ACS Nano* **2015**, *9*, 7287−7295.
(45) Böckmann, H.; Liu, S.; Mielke, J.; Gawinkowski, S.; Waluk, J.; Grill, L.; Wolf, M.; Kumagai, T. *Nano Lett.* **2016**, *16* (2), 1034−1041.
(46) Novko, D.; Blanco-Rey, M.; Tremblay, J. C. *J. Phys. Chem. Lett.* **2017**, *8*, 1053−1059.
(47) Mehlhorn, M.; Gawronski, H.; Nedelmann, L.; Grujic, A.; Morgenstern, K. *Rev. Sci. Instrum.* **2007**, *78*, 033905.
(48) Aizpurua, J.; Hoffmann, G.; Apell, S. P.; Berndt, R. *Phys. Rev. Lett.* **2002**, *89*, 156803.
(49) Pettinger, B.; Ren, B.; Picardi, G.; Schuster, R.; Ertl, G. *J. Raman Spectrosc.* **2005**, *36*, 541−550.
(50) Meng, L.; Yang, Z.; Chen, J.; Sun, M. *Sci. Rep.* **2015**, *5*, 9240.
(51) Zrimsek, A. B.; Chiang, N.; Mattei, M.; Zaleski, S.; McAnally, M. O.; Chapman, C. T.; Henry, A.-I.; Schatz, G. C.; Van Duyne, R. P. *Chem. Rev.* **2017**, *117*, 7583−7613.
(52) Chen, C. J. *Introduction to Scanning Tunneling Microscopy*, 2nd ed.; Oxford University Press: Oxford, 2008.
(53) Neacsu, C. C.; Steudle, G. A.; Raschke, M. B. *Appl. Phys. B: Lasers Opt.* **2005**, *80* (3), 295−300.
(54) Behr, N.; Raschke, M. B. *J. Phys. Chem. C* **2008**, *112* (10), 3766−3773.
(55) Winsemius, P.; Kampen, F. F. v.; Lengkeek, H. P.; Went, C. G. v. *J. Phys. F: Met. Phys.* **1976**, *6*, 1583−1606.
(56) Liljeroth, P.; Repp, J.; Meyer, G. *Science* **2007**, *317*, 1203−1206.
(57) Auwärter, W.; Seufert, K.; Bischoff, F.; Ecija, D.; Vijayaraghavan, S.; Joshi, S.; Klappenberger, F.; Samudrala, N.; Barth, J. V. *Nat. Nanotechnol.* **2011**, *7*, 41−46.
(58) Kumagai, T.; Hanke, F.; Gawinkowski, S.; Sharp, J.; Kotsis, K.; Waluk, J.; Persson, M.; Grill, L. *Phys. Rev. Lett.* **2013**, *111*, 246101.
(59) Kumagai, T.; Hanke, F.; Gawinkowski, S.; Sharp, J.; Kotsis, K.; Waluk, J.; Persson, M.; Grill, L. *Nat. Chem.* **2013**, *6*, 41−46.
(60) Ladenthin, J. N.; Frederiksen, T.; Persson, M.; Sharp, J. C.; Gawinkowski, S.; Waluk, J.; Kumagai, T. *Nat. Chem.* **2016**, *8*, 935−940.

DOI: 10.1021/acs.nanolett.7b03720
Nano Lett. 2018, 18, 152−157